CHALMERS UNIVERSITY OF TECHNOLOGY
SE-412 96 Gothenburg, Sweden
Telephone: +46 (0)31 772 10 00
www.chalmers.se

Ungefär 100 kilo ATP syntetiseras i kroppen varje dag av ATP-syntas, ett sammansatt proteinkomplex med tre aktiva centra. Komplexet sitter förankrat i ett biologiskt membran med hjälp av hydrofob attraktion och består av en roterande och en statisk del. En ATP-molekyl syntetiseras per tredjedels varv. Trots att varje aktivt centrum skulle kunna fungera oberoende av de andra, sparas mycket energi av att de enskilda reaktionerna fördelas jämnt över tiden. I artikel 6 i denna avhandling kallar vi detta fenomen för ”katalys genom fasförskjutning”.

Hydrofob (av ὕδωρ, ’vatten’ och φόβος, ’fruktan’) attraktion sker mellan biomolekyler i lösning för att minimera ytan som är exponerad för vatten. Hydrofob attraktion håller samman DNA-strängar, lipidmembran och proteinkomplex, och kan användas för att binda proteiner till DNA och förankra DNA till membran.

Denna avhandling handlar om hydrofoba krafter ur ett biologiskt och nanotekniskt perspektiv, med utgångspunkt i DNA-strängutbyte. Genom strängutbyte skapas nya dubbelsträngar genom tillsats av enkelsträngar (se Fig. 6), en process som katalyseras av hydrofob växelverkan mellan DNA och dess omgivning. Målsättningen med forskningen som presenteras i denna avhandling är att bättre förstå hydrofoba krafters roll i till exempel reparation av felaktiga DNA-baser och konstruktion av membranbaserade nanosystem.

BOBO FENG

CHALMERS

BOBO FENG

DNA strand exchange and hydrophobic interaction between biomolecules

2015

CHALMERS

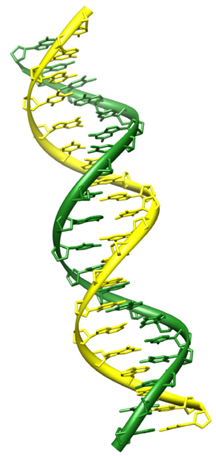

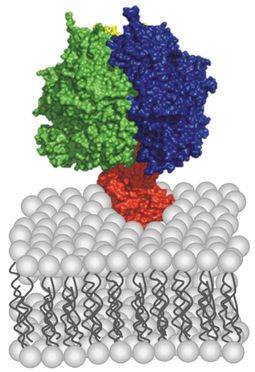

DNA strand exchange and hydrophobic interactions between biomolecules

BOBO FENG

Department of Chemistry and Chemical Engineering
CHALMERS UNIVERSITY OF TECHNOLOGY
Gothenburg, Sweden 2015

THESIS FOR THE DEGREE OF DOCTOR OF PHILOSOPHY

DNA strand exchange and hydrophobic interactions between biomolecules

BOBO FENG

Department of Chemistry and Chemical Engineering

CHALMERS UNIVERSITY OF TECHNOLOGY

Gothenburg, Sweden 2015

DNA strand exchange and hydrophobic interactions between biomolecules

Bobo Feng

ISBN 978-91-7597-176-6

Doktorsavhandlingar vid Chalmers tekniska högskola
Ny serie nr 3857
ISSN 0346-718X

Department of Chemistry and Chemical Engineering
Chalmers University of Technology
SE-412 96 Gothenburg
Sweden

Telephone + 46 (0)31-772 1000

Cover image:
Hydrophobic attractions are essential for the structure and function of biomolecules. Left: The two strands in a DNA helix are joined by base stacking in an aqueous environment (section 2.1). Right: ATP synthase inserts itself into a lipid bilayer, with the F_1 portion above the membrane (paper 6).

Chalmers Reproservice
Gothenburg, 2015

Abstract

The role of hydrophobic interactions in DNA strand exchange has been studied using fluorescence-labeled DNA oligomers in a FRET assay. Strand exchange was found to be accelerated in the presence of polyethylene glycol, which provides a crowded and hydrophobic environment possibly mimicking that of the catalytically active recombinase-DNA complexes. Circular dichroism spectroscopy shows that B-DNA conformation is conserved, so the increased rate of exchange is not simply caused by melting of DNA duplexes. A hydrophobic environment increases the base pairing accuracy of DNA strand exchange, which causes mismatched duplexes to quickly be replaced in the presence of matching strands. It is inferred that these effects are caused by a decrease in water activity which weakens the DNA stacking forces, and by favorable hydrophobic interactions between PEG and DNA chains, with the result that DNA breathing and subsequent strand invasion is facilitated.

Linear dichroism and dynamic light scattering were also used to study some other biomolecular systems where hydrophobic interactions are important: lipid membranes, DNA-protein complex, DNA nanoconstructs anchored to membrane surface, and to study fusion of liposomes induced by shearing forces. A DNA hexagon construct was found to adopt different orientations at the membrane surface depending on the number of attached anchors, but the construct itself was inferred to have a metastable shape due to internal flexibility. Finally, an example of assembly of protein subunits to a membrane surface was considered in shape of the ATP synthase system for which we propose that the activation energy of ATP synthesis may be reduced through coupled reactions between three active sites. The results are interesting in more general contexts of methodological improvements for studying biomolecular assembly, including linear dichroism spectroscopy of transmembrane proteins.

Keywords: Hydrophobic interactions, self-assembly, DNA, strand exchange, linear dichroism, nanotechnology, liposomes, ATP synthase, membrane proteins

List of publications

This thesis is based on the results of the following appended publications:

Paper 1 DNA strand exchange catalyzed by molecular crowding in PEG solutions
Bobo Feng, Karolin Frykholm, Bengt Nordén, and Fredrik Westerlund
Chemical Communications, 2010, 46.43: 8231-8233.

Paper 2 Evidence for hydrophobic catalysis of DNA strand exchange
Bobo Feng, Fredrik Westerlund, and Bengt Nordén
Accepted for publication in Chemical Communications

Paper 3 Sequence specificity of DNA strand exchange and the hydrophobic environment effect
Bobo Feng and Bengt Nordén
Manuscript

Paper 4 Controlling and monitoring orientation of DNA nanoconstructs on lipid surfaces
Erik Lundberg, Bobo Feng, Amir Saeid Mohammadi, Marcus Wilhelmsson, and Bengt Nordén
Langmuir, 2012, 29.1: 285-293.

Paper 5 Shear-Induced Membrane Fusion in Viscous Solutions
Maxim Kogan, Bobo Feng, Bengt Nordén, Sandra Rocha, and Tamás Beke-Somfai
Langmuir, 2014, 30.17: 4875-4878.

Paper 6 Energy phase shift as mechanism for catalysis
Tamás Beke-Somfai, Bobo Feng, and Bengt Nordén
Chemical Physics Letters, 2012, 535: 169-172.

Paper 7 UV Transition Moments of Tyrosine
Louise Fornander, Bobo Feng, Tamás Beke-Somfai, and Bengt Nordén
The Journal of Physical Chemistry B, 2014, 118.31: 9247-9257.

Contribution report

Paper 1	Designed and performed the experiments, and wrote the paper.
Paper 2	Designed and performed the experiments, and wrote the paper.
Paper 3	Designed and performed the experiments, and wrote the paper.
Paper 4	Designed and performed some of the experiments, finished the paper from a manuscript.
Paper 5	Participated in designing, experiments, and writing the paper. The lipid mixing fluorescence assay mostly the work of SR.
Paper 6	Participated in designing, calculations, and writing the paper.
Paper 7	Designed and performed most of the calculations. Experiments mostly the work of LF. Assisted in writing the paper.

Table of Contents

1 Introduction

A polyvalent cation, such as polyarginine, will bind to DNA through electrostatic attractions. The DNA will condense, or if the concentration is sufficient, aggregate until it precipitates out of the solution. However, when the recombination enzyme RecA interacts with single stranded DNA to mediate homologous recombination, it does not bind by simple ionic attraction. One protein unit of RecA after another covers the DNA until a tight protein-DNA complex is formed. Strong protein-protein interaction makes the process highly cooperative and, furthermore, the DNA bases are separated from each other in triplets, with the gaps filled with hydrophobic amino acid residues.

Through mechanisms which are yet not understood, the complex searches for homology between the single DNA strand and an entering double-stranded DNA helix. In case of encountering homology, the single strand invades the helix, and a new DNA duplex is formed. Two intriguing questions are: why must the nucleobase-nucleobase stacking be broken, and why is it easier for a single strand to invade a double strand when it is covered by bulky proteins?

Throughout scientific history, answering 'how?' carries more prestige than answering 'why?'. Being able to tell *how* currents may flow in electrical circuits, from plus to minus, has enabled various electrical applications, but discovering *why* (because the electrons are negatively charged and actually move in the opposite direction) did not cause the electrical schemes to be redrawn. Keeping the existing convention was more important.

This thesis tries to make an attempt to investigate why hydrophobic interactions are ubiquitous to the function of biomolecules, using DNA strand exchange as a starting point and a model system. The discovery in Paper 1, that strand exchange of short DNA oligomers is catalyzed by polyethylene glycol, is re-visited in Paper 2 which shows that polyethylene glycol also increases the base pairing accuracy of DNA, and in Paper 3 which tries to explain the effect using hydrophobic interactions as an argument.

The thesis discusses several examples of interactions between DNA, proteins, and membranes, driven by the hydrophobic effect. In Paper 4, the anchoring of a self-assembled DNA nanoconstruct to a lipid membrane is controlled and measured. In Paper 5 focus is on liposome fusion, one way of joining different lipid membranes. Another way, in which DNA acts as membrane linkers, is included briefly in the results section, and may be used also to help to study membrane-bound proteins. In Paper 6, we approach theoretically by a simple mechanical cooperative model the function of ATP synthase, a membrane-bound enzyme complex central to life and energy conversion, which utilizes the economy of scale to overcome energy barriers. Lastly, the thesis also includes some methodological aspects on

how to study and manipulate biomolecules. Papers 1 to 4 have practical applications in the construction of DNA nanoconstructs. Papers 4 to 7 provide methods to study membrane-bound systems using linear dichroism (LD) spectroscopy, including membrane-bound DNA nanoconstructs and transmembrane proteins.

2 Background and theory

Living cells are surrounded by a **lipid membrane** enclosing **proteins** and **nucleic acids**, of which **DNA** is an example. A **liposome** is a spherical synthetic lipid membrane. A single DNA molecule (ssDNA) is a **single strand**; two single strands can form a helical **double stranded** form (dsDNA) through **base pairing**. DNA has its **sequence** defined by its constituent four **nucleobases,** if A·T and G·C base pairing fails, a **mismatch** is said to occur. The stability of a DNA duplex is most commonly characterized by its **melting temperature**, the temperature at which half of the original DNA duplexes have dissociated due to thermal activation.

DNA **strand exchange** occurs when a single strand **invades** a double strand and displaces one of its strands, creating a new double strand and a free new single strand (see Figure 6).

In this thesis, '**hydrophobic effects'** is a collective name for the influence from **nonpolar** molecules, and **hydrophobic attraction** which is caused by **desolvation**. '**Hydrophobic catalysis**' refers to catalytic activity caused by the nonpolar character of the **environment**. A high concentration of **macromolecules** can cause **molecular crowding**, which may be amplified through **volume exclusion**.

2.1 Biomolecules and hydrophobic attractions

The three main types of biomolecular aggregates: nucleic acids, lipid membranes, and proteins, all depend on hydrophobic attractions for their structure and function (see Figure 1). The nucleobases in DNA and RNA are *aromatic*; guanine alone is a molecule that is almost insoluble in water, and also the other four nucleobases (including uracil found in RNA) are only slightly soluble. The historical belief that the DNA double helix is held together by hydrogen bonds within base pairs has progressively become considered less correct[1, 2, 3, 4]. According to the old view, predicting the melting temperature of a DNA duplex from its sequence was based on the different number of hydrogen bonds between A·T (two) and G·C (three), which explained why the melting temperature increased with GC content. Meanwhile, the contribution from hydrophobic forces was given only a small correction factor. It was not immediately evident that the old view was problematic, because the temperatures were correctly predicted. Not until 2006 was it finally concluded that base stacking is the major contribution to DNA stability, while hydrogen bonding is a small correction factor[5, 6]. Hydrogen bonding in A·T is even destabilizing the DNA while G·C is energetically almost neutral when all other interactions are taken into account. The GC dependence of melting temperature can now be explained by the different base stacking capabilities of each nucleobase, while sequence selectivity of base pairing is mostly due to sterical reasons[7, 8].

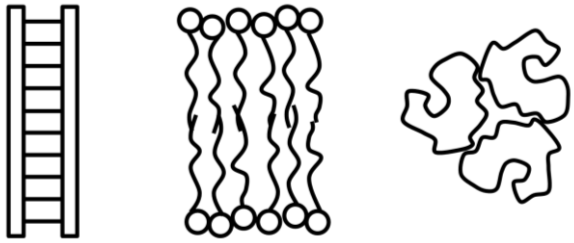

Figure 1. Schematic illustration of self-assembly of biomolecules due to hydrophobic attraction. Left: Two DNA strands are joined in a DNA duplex. Middle: Lipids spontaneously form a flat membrane. Right: Protein monomers assemble into a functional unit (although electrostatic attractions are usually also involved).

Base stacking occurs when free nucleotides are dissolved in water. Instead of base pairing, as was originally expected, they aggregate into what may be described as coin rolls.[9, 10] This phenomenon is caused mainly by electrostatic and desolvation effects, with some contribution from dispersion (London) electron correlation forces.[11, 12, 13, 14, 15, 16] Electrostatic attractions between stacked nucleobases are permanent dipole-dipole and dipole-induced dipole attractions due to electronegative atoms and polarizable electron clouds in carbonyl groups and aromatic rings. It should be noted that electrostatic attractions are studied using free molecules, but the individual nucleobases in B-DNA have limited freedom of movement and the actual overlaps are not ideal with respect to maximum attraction[17, 18]. The ideal overlap between localized charges between neighboring bases, using every possible combination of bases, must be geometrically different, but the B-DNA arrangement forces approximately the same rise and twist onto every base. As a further note, so called pi-pi stacking interactions (i.e. dispersion forces due to the high polarizability anisotropy of pi-electron clouds) were once thought as a special type of interaction between nucleobases. However, they are now found to be almost negligible, and not fundamentally different from other dispersion forces.[12, 19, 20]

Helix stabilization through desolvation refers to the advantage of burying the hydrophobic nucleobases of DNA in the center of the helix, instead of having them exposed to the aqueous solvent. A polar solvent such as water adopts a low-entropy, cage-like structure at a hydrophobic solute-solvent interface, so there is a large gain in free energy upon minimizing the total exposed surface area of the nucleobases. If the bulk water concentration is lowered, for example in a crowded cell nucleus, the contribution to helix stability will be lowered too. Several authors have stated, by computing electrostatic energy maps of molecular models of

nucleotides, that non-electrostatic interactions (desolvation and dispersion) are more important than pure electrostatic interactions.[21, 22] There is a brief review of the state of art of research in the 2006 article by Frank-Kamenetskii and coworkers[23], stating that authors have not agreed on the relative importance of electrostatic and hydrophobic contributions to base stacking, and a definitive answer is obviously yet to be found.

The importance of hydrophobic interactions is not limited to nucleic acids. Biological membranes are constructed of a lipid bilayer, with each lipid molecule having a hydrophilic head group and a hydrophobic tail. The same principles as for nucleic acids apply to the attraction between lipid molecules: hydrophobic desolvation and dispersion forces. The flat membrane shape provides minimum exposure of the hydrophobic tails to the surrounding aqueous environment, while keeping the polar head groups in contact with the water phase. Without the head groups, the membrane would collapse into a spherical oil droplet.

The lipid membrane is essentially a two-dimensional nonpolar phase in water solution, and as such can be used to enrich a wide range of hydrophobic targets. Small molecules simply insert themselves between the hydrophobic tails, while larger molecules are anchored to the surface, for example via a hydrophobic anchor molecule. In Paper 4 of this thesis, DNA nanoconstructs are anchored to a liposome surface using fatty acid anchors[24]. In Paper 5, retinoic acid is used as a lipophilic probe which is inserted into the membrane itself[25]. In Paper 6, we study the energetics of an enzyme complex inserted into and spanning across a lipid membrane[26]. In all of these cases, hydrophobic interactions maintain the structure of the respective system and provide basis for how solutes are solubilized.

2.2 DNA nanotechnology and self-assembly

DNA base-pairing accuracy is a balance between two requirements. Inheritance of genetic information through DNA replication requires a high level of fidelity, but the process of natural selection requires also some mismatching to accidentally occur (mutation). Life as we know it will require a mismatch rate of no more than a few mismatches per million base pairs.[27, 28] However, such a small rate is maintained by error-checking proteins *in vivo*. By contrast, under laboratory conditions mismatched duplex DNA is easily created with a melting temperature penalty of very roughly one degree per percent mismatch, depending on sequence, DNA concentration and salt concentration.[29, 30]

The ability of sequence recognition makes DNA an ideal building block for nanosized structures. The various applications include mechanical devices[31], logical gates[32, 33], molecular motors[34, 35, 36], and chemical assembly lines[37, 38, 39] – a short overview of the more notable examples is given in Paper 4. The justification of using DNA to build bottom-up

nanosized devices, instead of other techniques such as top-down lithography, is that DNA will automatically by thermal diffusion self-assemble into the desired structure in aqueous solution. The final 3D-structure is uniquely defined once the DNA sequence has been designed. Therefore miniaturization and functionalization of DNA nanodevices rely on currently available methods for chemical synthesis, and therefore is a complementary method to photolithography, which itself could depend on a preformed DNA template[40, 41].

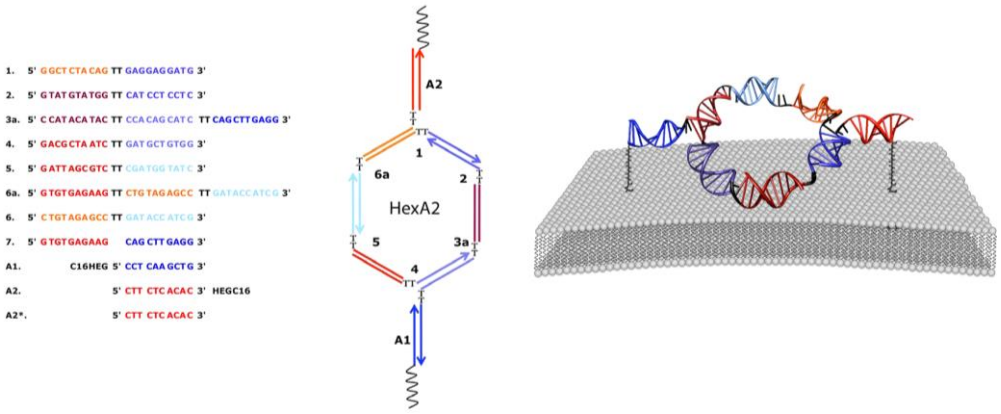

Figure 2. HexA2 DNA hexagon (from Paper 4) is built from synthetic strands (left) which will self-assemble to a ring structure (middle), and two lipid anchor chains, that will insert themselves into a lipid membrane (right). The process is mainly driven by hydrophobic attraction between nucleobases and between lipids. In case the membrane carries positive charge, also electrostatic attraction contributes.

The construction of a DNA nanodevice relies on hydrophobic attraction between staggered DNA strands, see Figure 2. The depicted DNA hexagon might also be inserted into a lipid membrane through hydrophobic attraction, provided its backbone is modified to make it hydrophobic, and similar hexagons can be extended into a network[42] or functionalized with fluorophores[43, 44]. Unlike so-called DNA origami, which is folding a long piece of DNA into a static geometric shape, DNA-based molecular motors can transport other macromolecules and often rely on strand exchange with added DNA as a "fuel"[34, 35, 36, 45, 46, 47]. The strand exchange can be designed to cause an overall conformational change resulting in a corresponding molecular movement. As we argue in Paper 1, not only are hydrophobic effects important to the structure of these devices, increasing the speed of strand exchange will also improve the efficiency of such dynamic nanodevices.

2.3 Molecular crowding

Another example of role of hydrophobic forces in action is the binding of recombination enzymes, like RecA, to DNA – involving cooperative protein-protein attraction. The first three papers in this thesis investigate the importance of a crowded and hydrophobic environment for DNA strand exchange. In a crowded environment, macromolecules (like DNA) can make closer contact with co-solutes (like PEG) without any solvent (like water) molecules in between. A good example of a crowded environment is the cytoplasm of the cell, which can contain 40 % (by volume) dissolved macromolecules.[48] An even more extreme example is the RecA-DNA complex during homologous recombination, in which three DNA strands are simultaneously bound by surrounding repeating RecA units in a compact, elongated helical fiber structure.[49]

Molecular crowding has been found to have significant general impact on the structure, stability, and function of nucleic acids and proteins.[50, 51, 52, 53, 54, 55] In crowded environments, hydrophobic interactions become an important factor in determining the structure and function of biomacromolecules. Firstly, overall water activity is reduced by the presence of the co-solutes, which bind water molecules in a shell of solvation. Secondly, the co-solutes can make themselves direct contact with the solute of interest, and thus exposing the solute to a hydrophobic environment, even though the majority of the co-solute is hydrophilic enough to remain in solution. These effects are generally not encountered when biomacromolecules are studied in dilute water solutions, in which they keep their native conformation despite that they lack their native environment.

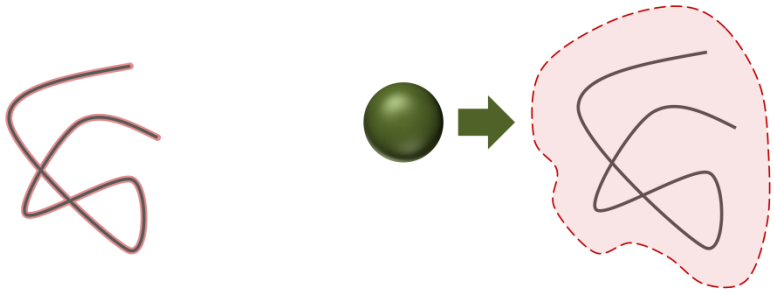

Figure 3. The difference between the volume of a long and thin macromolecule (left), and its effective volume of exclusion (right). The volume of exclusion is often estimated using the radius of the molecule of interest (green). The center of the molecule of interest cannot occupy any of the excluded volume.

Molecular crowding, which is a physical description of state, can occur due volume exclusion, a geometrical effect[56, 57]. Intuitively, but incorrectly, the concentration of a solute of interest

may seem doubled if half of the reaction volume is occupied by inert co-solutes. A more correct model must take the three-dimensional shape of the solutes into account. Especially, long and thin macromolecules create a volume of exclusion, into which other reasonably large molecules are not allowed due to steric hindrance, significantly larger than the volume of the macromolecule itself (see Figure 3). Smaller molecules, which approach the solvent molecules in size, cannot generate a volume of exclusion because they cannot exert sufficient steric resistance against other macromolecules. In Paper 3, different lengths of PEG are used in an attempt to isolate the effect of volume of exclusion from hydrophobic effects. When PEG length is decreased, the volume exclusion effect will also vanish. However, a shorter PEG molecule may retain all the other characteristics of longer PEG, including the hydrophobic character of PEG itself, and its ability to bind water molecules.

Polymers of significant molecular size, such as Ficolls, dextrans, and PEG (H-[-O-C_2H_4-]$_n$-OH), are often used as inert co-solutes to study biomolecules in solution. While the first two are based on sugars and therefore hydrophilic (dextran is being marketed as 'extremely hydrophilic'), PEG has significant hydrophobic character due to its -C_2H_4- fragments. Similar polymers, including both the -CH_2- and -C_3H_6- structural analogs, are considered too hydrophobic to be water soluble. It is thought that PEG solubility in water depends on the precise oxygen-oxygen distance, which enables water molecules forming a cage-like structure surrounding the polymer[58, 59, 60, 61, 62]. As a result, we propose PEG can be used as a hydrophobic DNA-compatible crowding agent, although it exhibits some specific interactions with proteins[56].

The limited volume constraint in crowded solutions dominates over entropy effects, which means that aggregation and self-assembly reactions are favored. Two good examples of cooperative effects in enzyme activity are the binding of RecA to DNA[63, 64, 65] and the self-assembled ATP synthase complex[66, 67] both kinds of systems involving problems that are considered in this thesis. However, it should be noted that DNA strand exchange among matching strands of equal length carries no net change in entropy, and nor is it favored by any geometrical aspects of molecular crowding.

3 Concepts and methods

In this section, the main experimental and computational methods will be presented, along with a brief description of the theory behind polarized spectroscopy.

3.1 Linear and circular dichroism

Sometimes it is forgotten that absorption in the ultraviolet and visible regions is a polarized-light phenomenon, the electric field of the radiation field always being perpendicular to the propagation direction. According to the Bohr frequency condition $\Delta E = h\nu$, radiation is absorbed if its energy $h\nu$ matches the energy difference ΔE between two concerned electronic, vibrational, or rotational states of a molecule. The electric transition dipole moment μ_T for a transition between states Ψ_i to Ψ_f is given by

$$\mu_T = \int \Psi_f^* \mu \Psi_i \, d\tau$$

where μ is the electric dipole operator. The probability P of absorption of a photon is then according to Fermi-Dirac's "golden rule"

$$P = \frac{1}{h} \left| \int \Psi_f^* V \Psi_i \, d\tau \right|^2 \rho$$

where ρ is the density of final states. Since the interaction energy V between the photon-electric field E and μ is $V = |E \cdot \mu|^2$, we have

$$A \propto |\mu_T|^2 \cos^2 \theta$$

where θ is the angle between the transition dipole moment μ_T and the electric field E. If the transition dipole moments of individual molecules in a sample have a net orientation along some macroscopic axis (along either a positive or a negative direction, since μ_T is a vector quantity), this sample will exhibit a net preferential absorbance of light polarized along that axis.[68]

Polarized light absorption is the basis for linear dichroism (LD) spectroscopy, in which molecules are aligned along a macroscopic axis, using for example shear flow, stretched films or electrostatic fields, and subject to light polarized alternatively horizontally or vertically relative to that axis. Linear dichroism is defined as

$$LD = A_{parallel} - A_{perpendicular}$$

so that LD has a positive sign if the transition dipole moments of the molecules are aligned along the macroscopic reference axis and negative when perpendicular to it. In Paper 7 of this thesis, *para*-cresol is aligned using a stretched film in the horizontal direction which is taken as the macroscopic axis. The L_b transition (Platt's nomenclature[69], absorption at 200-300 nm) will show negative LD since its transition dipole moment is perpendicular to the macroscopic orientation axis (see Figure 4). The angle α between the transition dipole moment and the macroscopic orientation axis under uniaxial orientation conditions can be expressed using the quantity 'reduced LD', according to

$$LD_r = \frac{LD}{A_{iso}} = \frac{3}{2} S\left(3\cos^2 \alpha - 1\right)$$

where A_{iso} is the absorbance of the same unoriented, isotropic sample, and S is an orientation factor which is 1 for a perfect orientation and 0 for an isotropic sample.

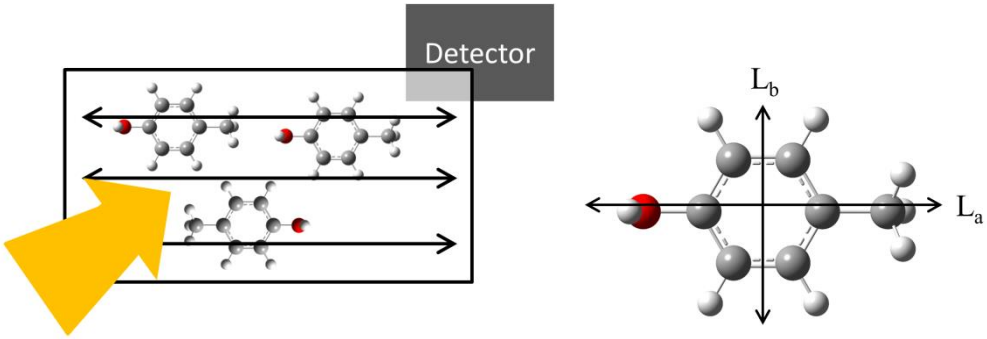

Figure 4. Left: schematic preferred alignment of p-cresol molecules in a stretched film. The horizontal axis is the macroscopic axis of orientation. Horizontally (parallel) and vertically (perpendicular) polarized light shines through the film into the detector. Right: L_a and L_b transition dipole moments of *p*-cresol. The L_b transition (250-300 nm) thus absorbs vertically and shows negative LD, while L_a (~200 nm) absorbs horizontally shows positive LD.

A couette cell can be used to orient liquid samples, for example DNA strands in solution. The sample is subject to shear forces between a rotating outer quartz cylinder and a stationary inner cylinder, which orients the molecules horizontally according to their hydrodynamic long-axis. The LD of double-stranded DNA has a negative peak at 260 nm in a couette cell, since the DNA strands are oriented horizontally, but the planes of the absorbing nucleobases in the stacked double helix are oriented perpendicular to this direction (see Figure 5).[70]

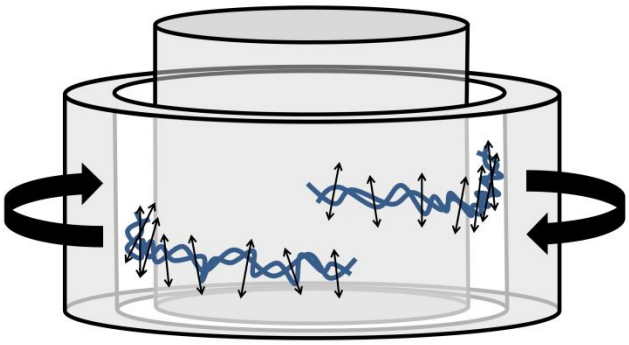

Figure 5. DNA aligned by shear forces in a rotating couette cell (the center cylinder is kept stationary). The transition dipole moments of the nucleobases are indicated, giving a net negative LD at 260 nm. For clarity, transition dipole moments 'inwards' the center of the cell are not shown.

Liposomes can be aligned in a couette cell and studied with LD using the same method, provided that a suitable hydrophobic LD probe, such as retinoic acid, is added and integrated into the membrane. Ideally, the chromophore adopts the same orientation as the lipid molecules so that the absorption of the chromophore is polarized along the membrane normal. When subjected to shear forces, the liposomes become elongated to give a net absorbance polarization in the vertical direction, which can be detected as a negative LD. An in-depth description of the theory behind LD spectroscopy, as well as the instrumentation and procedures, can be found in the 2010 book[68] by Nordén et al.

Circular dichroism is measured on an isotropic sample, and is defined as absorption difference between left and right circular polarized light:

$$CD = A_L - A_R$$

A sample may display CD activity if it contains an enantiomeric excess of a chiral molecule. The difference in absorbance can either be from the chiral molecule itself, or be induced into an achiral molecule by the complexation with a chiral one. The CD of DNA is caused by the helical stacking of nucleobases which in turn is dictated by the chirality of the sugar phosphate backbone. The shape of the CD spectrum is very sensitive to the conformation such as the pitch of the nucleobase stack, and may therefore be used as a structure-fingerprint. In this thesis, CD is used mainly to verify the conformation of B-DNA and to probe DNA melting.

3.2 DNA strand exchange

In principle, DNA strand exchange requires three steps. Firstly, the single strand must approach the double strand through diffusion. Secondly, somewhere along the sequence, a strand contact nucleation event occurs and a few nucleobases are exchanged. Lastly, strand exchange propagates along the DNA strand and one of the old strands in the duplex is ejected as a single strand. DNA strand exchange *in vivo* is catalyzed by the binding of the bacterial recombination enzyme RecA or its eukaryotic homolog Rad51. Several *in vitro* attempts to catalyze strand exchange, using charged polymers[71, 72] and liposomes[73, 74], have relied on multiple cationic charges to attract the DNA, reducing the dimensionality of the diffusion step. For example, in the case of liposomes, an increased probability of DNA molecules to encounter is due to a decrease from 3 dimensions to a 2-D planar surface.

There are mainly two issues of charge-based catalysis which can be addressed and further improved, as we note in Paper 1: Firstly, polycations tend to distort the DNA conformation and, therefore, cannot be used in a nanotechnological setting. Secondly, concentrated cationic charges probably do not truly reflect the crowded and hydrophobic environment found in the DNA-recombinase complexes. In this thesis, we believe that a nonionic catalyst may better mimic the conditions inside the recombinase and provide a deeper understanding of the DNA strand exchange mechanism and, thus, have wider practical applications.

Instead of directly studying strand exchange catalyzed by enzymes, which do not allow large variations in experimental settings, this thesis uses synthetic DNA strands as a model system. Two complementary DNA strands are labeled with FAM and TAMRA; which are two, respectively, fluorescein and rhodamine derivatives. The strands (3'-GCA GTT GTA TGT ATA GTG GT-5'-FAM and 5'-CGT CAA CAT ACA TAT CAC CA-3'-TAMRA) form a duplex, and a third strand, which is identical in sequence to the TAMRA strand but unlabeled, is added five times in stoichiometric excess.

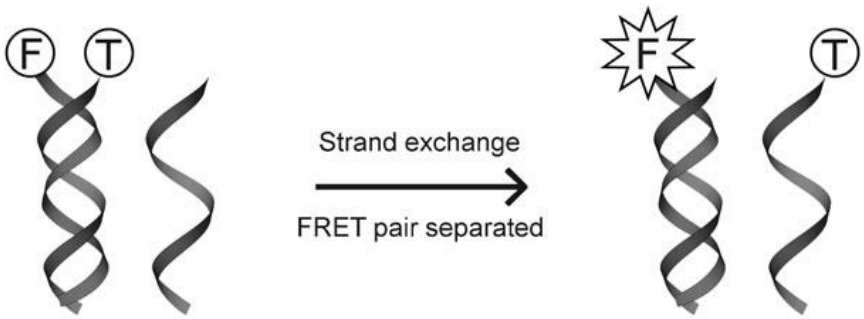

Figure 6. The principle behind FRET-based strand exchange assay, in which recovery of FAM fluorescence is directly proportional to the exchange yield.

In the original duplex, FAM is quenched through Förster resonance energy transfer (FRET) due to the proximity to TAMRA. Upon strand invasion by the third strand, the FRET pair is separated and FAM fluorescence is recovered (see Figure 6). FRET is a non-radiative energy transfer through space due to dipole-dipole coupling with a very strong dependence on distance according to

$$E = \left\langle \frac{1}{1+(r/R_0)^6} \right\rangle$$

where E is the energy transfer efficiency and R_0 is the characteristic "Förster" distance (normally in the range of 2-6 nm) which also depends on the fluorophores and their relative orientation. FRET can be seen as a binary on/off probe due to its strong distance dependency, and therefore the increase in FAM fluorescence is directly proportional to the yield of strand exchange. 0 % yield is normalized to the background FAM fluorescence in the absence of the third strand, while 100 % yield can be normalized using two different methods. Either 100 % yield is taken as the equilibrium fluorescence intensity, or the sample is heated above the melting temperature of DNA and then cooled, which causes equilibrium to occur. In practice, the two different methods yield the same result. A pseudo-first order rate constant *k* can be fitted to the fluorescence kinetics trace, according to the equation

$$I(t) = I_\infty - Ae^{-kt}$$

where I_∞ represents the equilibrium fluorescence intensity.

3.3 Quantum mechanical calculations of transition dipole moments

Light spectroscopy (FRET, CD or LD) is the method of choice for protein complexes whose structures in solution cannot be studied using crystallography or NMR methods, such as membrane bound proteins or aggregated protein filaments. Often knowing the exact orientations of the individual transition dipole moments becomes essential, for example when studying proteins using the Site-Selected LD by Molecular Replacement (SSLD-MR) method[75], when the LD spectra of mutated and wild-type proteins are compared against each other. In Paper 7, we compute the orientations of the electronic excitations of *p*-cresol (4-methylphenol), which is the chromophore of the amino acid tyrosine.

In this thesis, molecular structures and excitation energies are calculated using DFT (density functional theory, for calculating ground states of molecules) and TDDFT (time dependent density functional theory, for calculating excited states of molecules) using the software suite Hyperchem 8. "Density" here refers to electron density of a molecule; DFT methods rely on

computing the energy and properties of a molecule by first computing its electron distribution, instead of computing approximations to the wave functions which is very time-costly. The distributions are described using Gaussian functions of electron density, which linearly combine into approximations of atomic orbitals, and which orbitals are grouped into basis sets. The basis set used in this thesis to compute structures was 6-31+G(d,p), while the slightly more complex 6-31++G(d,p) was used for excitation energies. Both sets are commonly used in calculations of organic molecules, and take into account long-range interactions and electronic polarizability.

To accurately describe the effect of solvent (water, cyclohexane or methanol) on p-cresol, an explicit model was used in addition to an implicit solvent model (IEFPCM). An implicit model treats the solvent as a continuum with a specific dielectric constant to model the polarity of the surrounding molecules, while an explicit model also contains molecules of the actual solvent to account for effects such as hydrogen bonding.

4 Results

This thesis is based on seven appended papers: four on DNA, one on membranes, and two on proteins. Paper 2 is accepted for publication in Chemical Communications, Paper 3 is a manuscript, while the remaining papers are published. This section contains the rationale and summaries of results presented in the papers. Some relevant unpublished results, which are not included in any of the papers, are also presented.

4.1 DNA strand exchange in a hydrophobic environment

The common aim of the first three papers is to clarify the role of hydrophobic interactions on DNA strand exchange. In Paper 1, we present the initial discovery that DNA strand exchange is catalyzed by the presence of PEG-6000 as a co-solute in an aqueous solution. In Paper 2, an increased sequence recognition ability of strand exchange in the presence of PEG is investigated, while in Paper 3, we try to understand the mechanism behind the accelerating effect of PEG. In Paper 3, we also introduce the term “hydrophobic catalysis”, since we can argue that hydrophobic interactions between DNA and a hydrophobic environment created by PEG is behind the mechanism of action. Due to variations in the manufacturing process, the length distribution of commercially obtained PEG can vary significantly. As explained in Paper 2, short PEG chains are by weight more effective than long PEG chains. Therefore, some of the kinetic traces and rate figures can vary slightly between papers.

As explained previously, the invasion of a single DNA strand into a preformed DNA helix is the basis of *in vivo* gene recombination and repair on a whole genome scale as catalyzed by recombinases, but such systems are complex and the experimental parameters are constrained. Therefore, labeled oligonucleotides are used in this thesis as a simpler model system for studying strand exchange.

As shown in Figure 7, strand exchange in the absence of PEG or other accelerating agents is very slow. Mainly because DNA by design is kinetically resistant to single strand invasions, but also due to slow diffusion of the invading strand into the immediate vicinity of the double strand. In Figure 7, the traces for PEG concentrations 45 % and above reach completion (and thus 100 % normalization intensity can be obtained independently of a heated-cooled sample), but in the absence of PEG, complete strand exchange will take several days and never reach completion in practice.

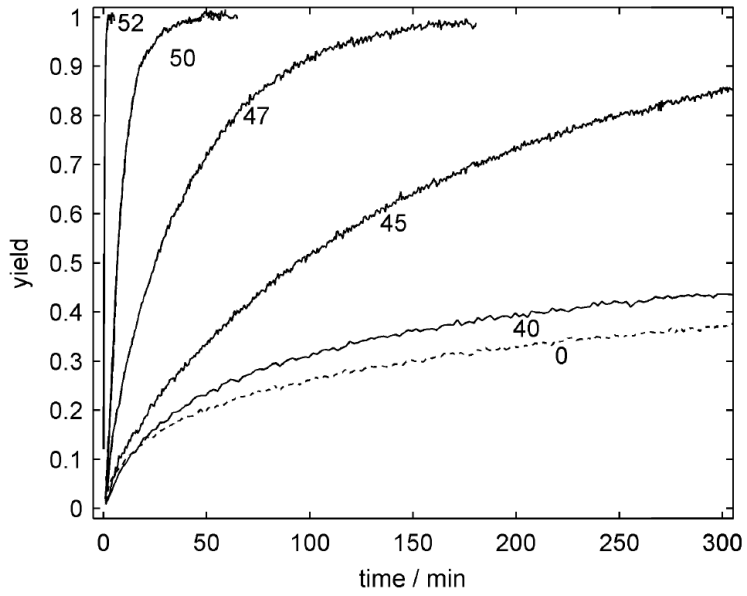

Figure 7. Kinetic traces over five hours of DNA strand exchange in the presence of 40 − 52 % PEG 6000 by weight (solid lines), compared to in the absence of PEG (pure buffer, dotted line).

The catalytic effect of PEG clearly depends very strongly on PEG concentration. While the actual difference in concentration between 40 % and 50 % may seem modest, the effects on strand exchange are hugely different. Whether this might be due to a phase change of the PEG-water system responding to increasing PEG concentration, could not be decisively excluded within the scope of this thesis, but could be considered unprobable. PEG in general requires a second polymeric cosolute to exhibit two-phase behavior, as evidenced in several cases [76, 77, 78] like the PEG/dextran phase separation. Some reports of phase inversion for PEG and various salts exist [79, 80], however, the sodium concentration used in this thesis is too small and no cloud point could be observed at the investigated concentrations.

It must be ruled out that the accelerating effect of PEG-6000 is not trivially due to some change in DNA conformation or in a decrease in duplex stability. Using CD spectroscopy in Paper 1, we could show that PEG does not lead to any significant deviations from the B-DNA helix, including possible conversion into psi-DNA. Also, salt was added to increase the melting temperature of DNA in the samples with PEG present, to exceed the melting point of DNA without PEG. The results show that the catalytic effect of PEG-6000 is not affected by the presence of additional salt and, therefore, comparing DNA in presence or absence of PEG is fair with respect to overall thermodynamics.

4.2 Increased strand exchange base pairing accuracy

The effect of a hydrophobic environment on DNA strand exchange with mismatches is further investigated in Paper 2 (unpublished manuscript). A 20-mer DNA duplex with one mismatched base is used instead of a fully matched duplex as in the previous paper. The mismatched duplex is converted through strand exchange into a fully matching duplex (see Figure 8): therefore, the process is analogous to DNA repair through homologous recombination. It could be argued that increasing the difference in speed between strand exchange between fully matched strands and between mismatched strands is equivalent to increasing the base pairing accuracy of DNA, since the end result is mismatched DNA being degraded and replaced with matching sequences.

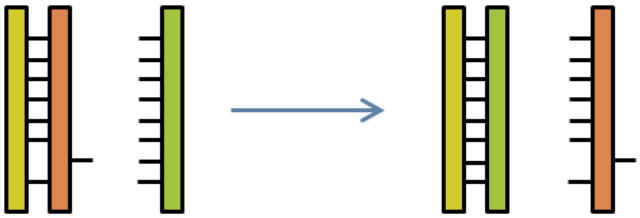

Figure 8. Repair of mismatched duplex DNA through strand exchange.

In the absence of PEG, the rate of disappearance of a mismatched duplex is only insignificantly greater than that of a fully matched strand. In the presence of PEG-6000, both the mismatched and the matched rates increase due to increased hydrophobicity (see Figure 9). However, the mismatched rate is 35 to 40 times higher than the matched rate. This difference could equivalently be expressed as the base pairing accuracy having increased in the presence of a hydrophobic environment caused by PEG. This is true no matter the position of the mismatch on the strand. However, since end fraying of the duplex is more likely than strand breathing in the middle of the duplex[81, 82], the increased accuracy caused by PEG was found to be more evident for a mismatch position at the end of the DNA for higher salt concentrations.

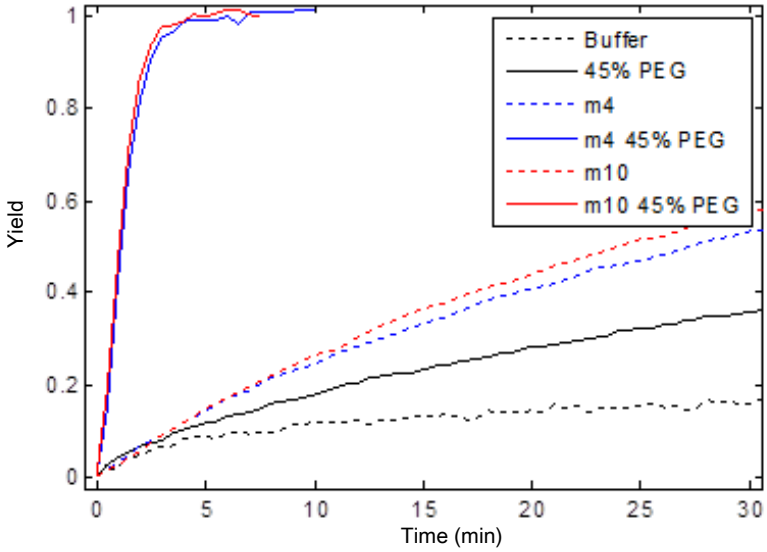

Figure 9. Mismatched (colored, m4 mismatch at the end, m10 in the middle of a 20 base sequence) and matched (black) strand exchange in the presence (solid) and absence (dotted) of 45 % PEG 6000. Obviously, the difference between mismatched and matched exchange is greatly amplified by PEG.

As expected, a mismatch ratio of 1/20 causes a drop in the melting temperature of DNA of about 6 degrees. To make the comparison between the rates of strand exchange justified, additional salt was added to the mismatched samples to “electrolytically compensate” for the loss in DNA helix stability caused by the mismatch. The added salt did not negate the increased base pairing accuracy; for mismatches close to one end, the rates were increased somewhat for moderate PEG concentrations, while for a mismatch in the middle, the rates were decreased. Taken together, the preference for mismatches close to the end of a DNA sequence might explain why recombination enzymes such as RecA break up the stacked nucleobases into short triplets, while the crowded and hydrophobic environment created by PEG mirrors the conditions at the interior of assembled DNA-enzyme filaments. If future research were to show that these speculations were true, considerable insight into the mechanism of RecA could be gained.

4.3 The mechanism of hydrophobic catalysis

Accelerating DNA strand exchange and increasing the base pairing accuracy of DNA are two effects caused by the presence of PEG as a co-solute. Since concentrated PEG solutions are strongly crowded and hydrophobic, several mechanisms of catalysis are possible. Since PEG polymers are widely used as crowding agents, it could immediately be suspected that an

"excluded volume effect" due to the sheer volume of PEG polymers concentrating the DNA into a smaller effective reaction volume. If this were true, then the trivial mechanistic explanation is simply that of shortening the required diffusion path length of DNA molecules and would be rather uninteresting. To investigate and, if possible disprove this, we studied strand exchange in the presence of short PEG chains and bulky but hydrophilic polymers in Paper 3. The four-carbon di-ether DME can be regarded as the shortest possible PEG chain, having the same structural elements as the longer PEG chains (and thus able of creating a hydrophobic environment) but not having any significant excluded volume effect being such a small molecule. Interestingly, DME was found to be even more effective than PEG in catalyzing DNA strand exchange. The hydrophilic polymers Dextran and Ficoll were also used to replace PEG, but no catalytic effect was observed with either of them. Therefore, it could be considered disproven that volume exclusion is a significant effect regarding catalysis of strand exchange.

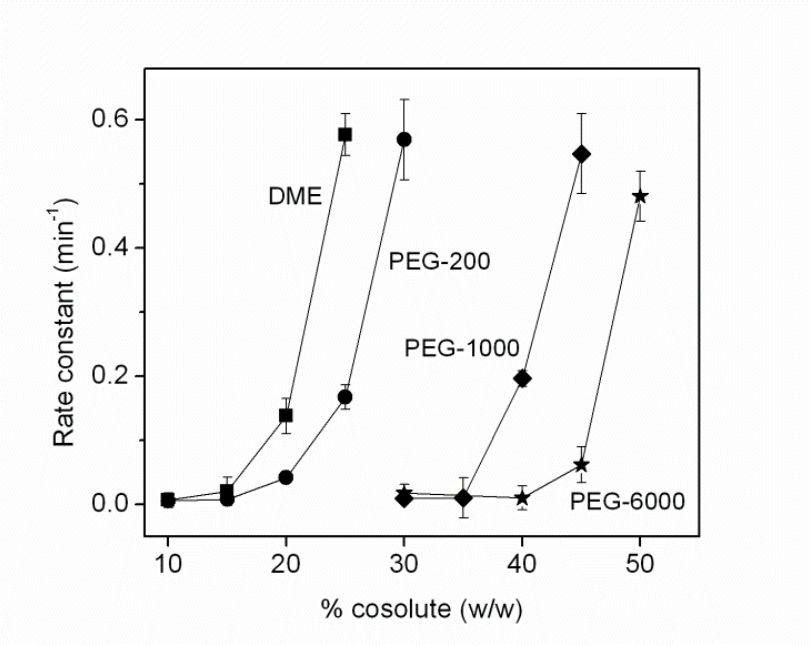

Figure 10. The rate constants of DNA strand exchange for different PEG lengths and concentrations.

By varying the lengths of PEG (Figure 10), and also changing the salt concentrations of the DNA samples, we could show that there are two major catalytic pathways, one salt-sensitive (catalytic effect vanishes with increasing salt concentration) and one salt-independent (see Figure 11). We propose in Paper 3 that the hydrophobic character of PEG, by decreasing the bulk water activity and providing favorable hydrophobic attractive forces between DNA and PEG chains, is responsible for the strand exchange catalytic activity. We show that a logical and consistent explanation is that DME and shorter PEG chains can enter the DNA grooves

and make hydrophobic close contact with the nucleobases, which disrupts base stacking (salt-sensitive pathway) and promotes strand breathing, which serves as nucleation points for strand invasion. In contrast, longer PEG chains are prevented due to sterical hindrance from making close contact, instead they may prolong strand breathing events by stabilizing the temporary single strands.

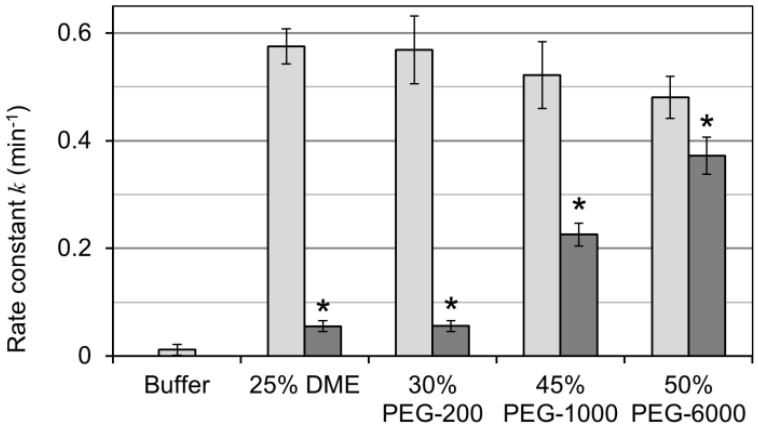

Figure 11. Effect of salt on the rate constant of strand exchange. An asterisk (*) indicates that salt was added to compensate for the loss of stability caused by a base mismatch. Longer PEG polymers retain more catalytic ability at high salt concentration than shorter PEG/DME.

4.4 DNA and liposome membranes

In Paper 4, we study DNA nanoconstructs anchored to a liposome surface using fatty acid chains, while the fusion dynamics of the lipid membrane itself is studied in Paper 5. The DNA hexagon with a side length of 10 bases was developed in our laboratory for use as a non-repeating addressable DNA network which can easily be functionalized (for example with fluorophores) through self-assembly by adding modified DNA oligomers.

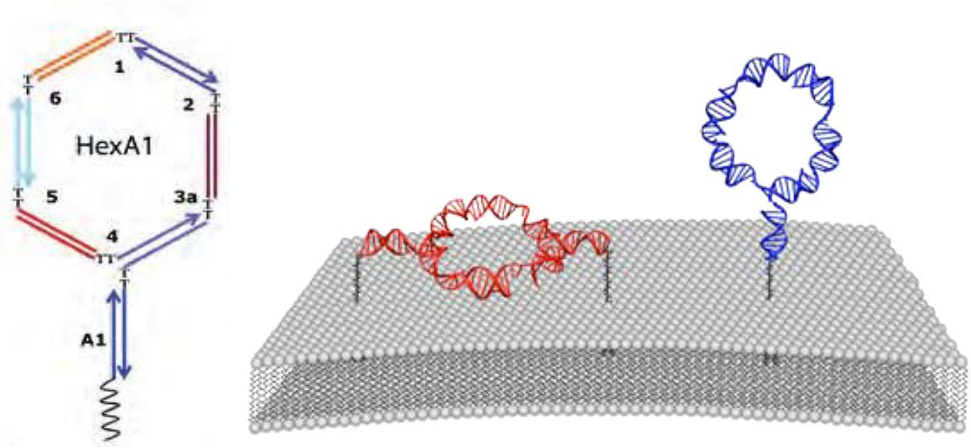

Figure 12. The DNA hexagon is self-assembled from individual DNA strands and anchored to the membrane surface using fatty acid chains. Either protruding (HexA1) or flat (HexA2) orientation is obtained by using one or two anchors.

In this case, being able to monitor the orientation of the nanoconstructs relative to the lipid surface using linear dichroism spectroscopy was more important than simply building the nanoconstructs. DNA hexagons have been anchored to lipid surfaces before, but LD could then never be used due to spectral overlap between the absorption spectra of DNA and porphyrins [83, 84]. A single anchor (HexA1) causes a protruding orientation with the LD spectrum being positive, while the opposite was true for two anchors (HexA2). We also found that the linker sequences alone (10-mer A1 in Figure 12, plus an equivalent 10-mer A1', plus a 20-mer single strand bridging both, 20 bp in total) gave the same LD spectrum as the entire construct. We believe this is because the DNA hexagon in reality is flexible or twisted instead of rigidly flat, and may adopt a variety of metastable shapes so that the LD contributions from each of them, or at least when averaged over all conformations, will average to zero.

We tried to calculate from LD and absorbance data the relative angle between the plane of the DNA hexagon and the membrane surface. Using the known dimensions of the nanoconstructs and liposomes, we could calculate the expected projected diameter of the covered liposome. This matched exactly the measured size of the liposomes using DLS for both of the orientations (Figure 13), a fundamentally different technique which verified that our conclusions about hexagon orientation were essentially correct.

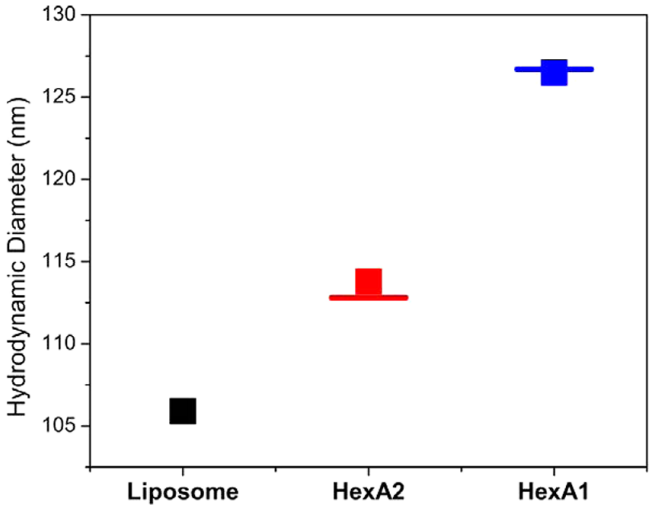

Figure 13. The sizes of covered liposomes obtained through DLS (colored squares) compared to bare liposomes (black square). The bars indicate the calculated size using LD data on the angle between nanoconstruct and membrane normal.

4.5 Aggregation and fusion of liposome membranes

One further development (unpublished data) from the study presented in Paper 4 was the fact that although no liposome aggregation was observed using the bi-anchored HexA2, extensive aggregation occurred if a bi-anchored 20 bp DNA construct (Figure 14) was used but, interestingly enough, only after activation through thermo-cycling which initially appeared very confusing to us. We eventually found that the short DNA construct, when added to free liposomes, preferentially attached itself with both anchors into the same liposome (out of proximity constraints) so then no aggregation occurs. Melting and re-annealing of the three constituent strands, however, causes the liposomes to become crosslinked by the DNA into a macroscopic aggregate (Figure 14). This process is virtually independent of path and arriving at the same result as a number of previous reports on DNA-crosslinked liposomes[85, 86] or even SNARE-like DNA (mimicking the function of liposome-fusing proteins) constructs[87, 88].

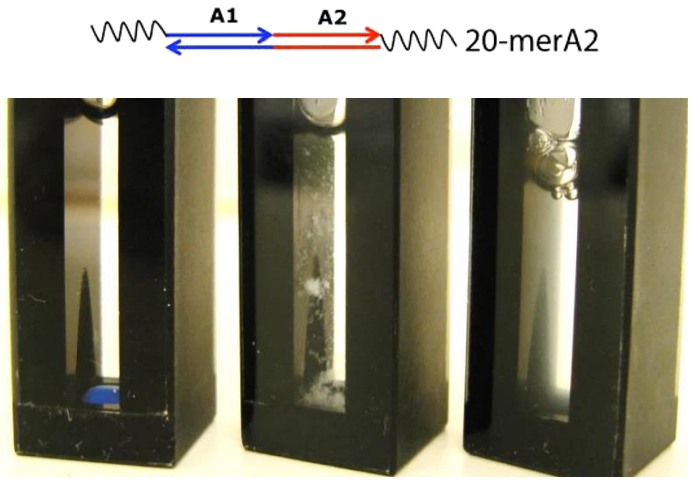

Figure 14. DNA-crosslinked liposomes. The bi-anchor DNA construct is shown schematically (DNA sequences in Paper 4). Left: Non-aggregated but DNA-covered liposomes before heat activation. Middle: Heavily aggregated liposomes after thermocycling. Right: Moderately aggregated liposomes after adding first the two anchors and then the bridging sequence in a one-pot reaction without heating.

To investigate whether crosslinked liposomes could be developed into a liposome-based drug delivery system, which was one of the future aims of the earlier articles, we encapsulated carboxyfluorescein into liposomes and then used DNA to crosslink them using the same experimental settings as presented in Paper 4. Large aggregates formed upon heat-activation (70 °C) as expected, while only trace amounts of carboxyfluorescein leakage were observed during the crosslinking process. These aggregates proved relatively resistant to low concentrations of Triton X-100 (about 0.2-0.5 % of the protocol concentration for complete membrane disruption) which was used to provoke total liposome leakage. Due to the crosslinked nature of the DNA/liposome aggregates, Triton could only affect the outermost layer of liposomes while the inner liposomes remained intact (Figure 15). These DNA-crosslinked liposomes proved capable of undergoing several thermocycles without leaking or changing their properties as confirmed by DLS, so in theory there remains the possibility of developing them into a drug delivery system with a payload released upon melting the DNA linkers through external heating.

An unsuccessful attempt was also made to dissolve the large liposome aggregates by adding the complementary strand of the 20-mer bridging strand, which is a milder (and probably smarter) treatment than heating. It was expected that the two short strands with lipid anchors (A1 and A2 in Figure 14) would be ejected as single strands through strand exchange. Although several concentration ratios between DNA and lipid were investigated, no

breakdown of the aggregates was observed. This was probably due to low penetration of the single DNA strand into the large aggregates, and slow strand exchange in the absence of a hydrophobic environment. No PEG was added since liposomes cannot remain stable when water activity is reduced. It is possible after future research that introducing mismatches into the short DNA construct to accelerate strand exchange will provide a workaround to this problem.

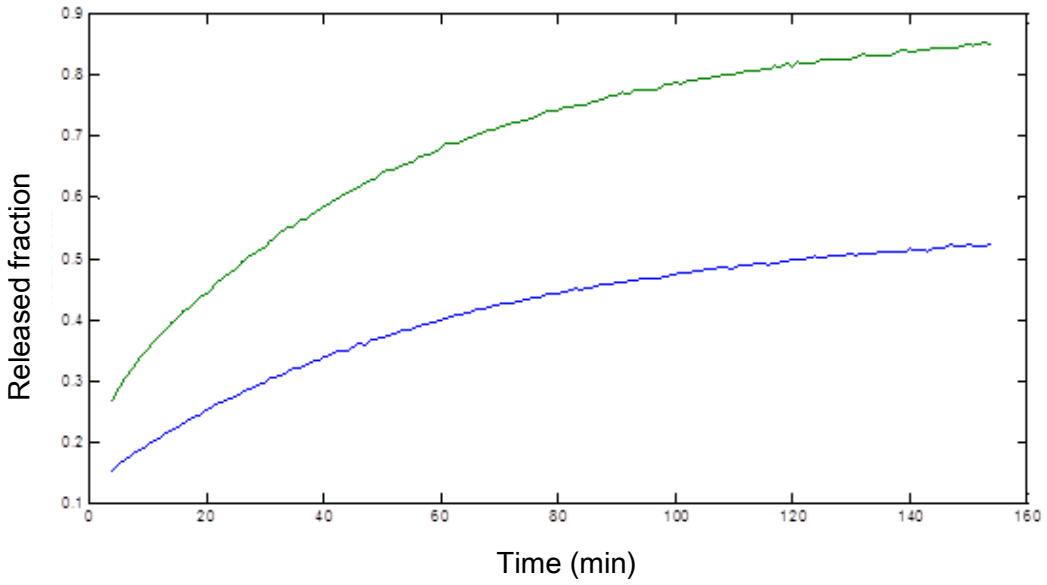

Figure 15. Triton X-100 induced leakage of carboxyfluorescein from aggregates (blue) and non-heat activated liposomes (green). While the individual liposomes release their carboxyfluorescein content over 3 hours, the clusters release only about half as much. Furthermore, the initial leakage from the addition of Triton is less for the liposome clusters.

Another method of joining liposomes is to fuse the membrane surfaces rather than aggregating them using cross-linkers. In Paper 5, therefore, we study the fusion of otherwise stable liposomes (extruded using DOPC lipids) by applying shear forces (shear rates above 3000 s^{-1}) in a linear dichroism flow cell. While providing better understanding over membrane dynamics, control over liposome fusion opens up new possibilities in creating lipid-based macromolecular assemblies. Retinoic acid was used as a lipid phase chromophore oriented perpendicularly to the lipid bilayer itself. We could observe over time an increase in the LD signal from retinoic acid which indicates a gradually better orientation of the chromophores, which ultimately could indicate a growth in liposome size. That this was a correct conclusion was verified using dynamic light scattering, which showed a growth in the

typical diameter of the liposomes from 100 pm up to 1000 pm, and also in parallel an increased polydispersity consistent with liposome fusion. To verify that membrane fusion (and not simply flocculation) has occurred, we also used the NBD-PE/Rh-PE couple of FRET quenching fluorophores attached to liposomes to show that the lipid bilayers were indeed fusing.[25]

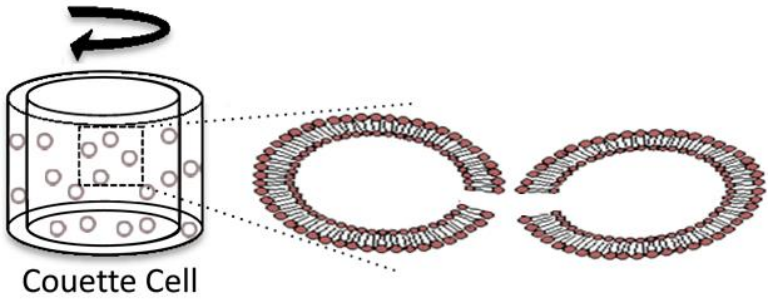

Figure 16. Conceptual model of membrane fusion caused by laminar flow shear force, inducing excessive deformation of vesicles which cause membrane disruption and fusion.

Sucrose was added to increase the viscosity of the sample, and over 30% sucrose (by weight) was required to achieve the desired effect (originally sucrose was introduced as a refractive index-matching agent to decrease light scattering in the LD spectrum of liposomes[89]). We therefore hypothesize that the membrane fusion is caused by mechanical stress causing excessive curvature in the membrane surface, which promotes fusion to minimize the excess surface energy (Figure 16).

4.6 Membrane-bound proteins

Paper 6 is a theoretical study of the conformational energetics of F_1 ATP synthase, while paper 7 concerns especially the study of orientable membrane proteins using linear dichroism. ATP synthase is a self-assembled enzyme consisting of several subunits anchored to a lipid surface, the mitochondrial inner membrane. The entire assembly can be considered a mechanical rotational engine on a tiny scale, either synthetizing ATP from ADP or, when in excess of ATP, expending ATP depending on the direction of rotation. The mobile part of the enzyme contains three active sites which are capable of independent activity. When coupled together mechanically as in the ATP synthase, the active sites must perform their chemical activity in a predetermined sequence, or essentially shifted with respective to each other in time.

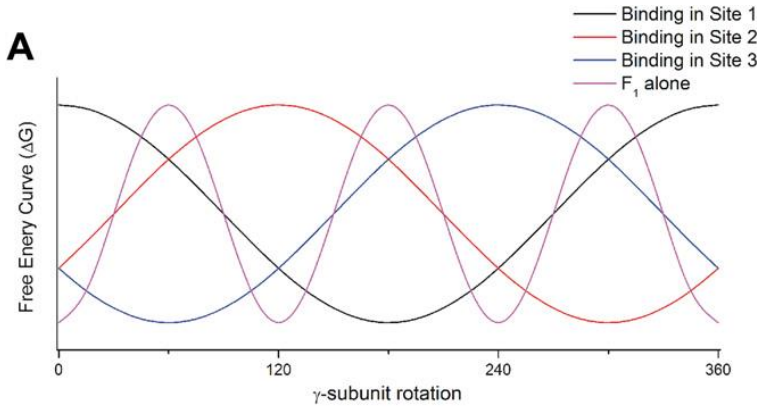

Figure 17. Conceptual graph of activation energy barriers approximated as sine waves, together with conformational energy ("F_1 alone"). The sum of the energies of the three sites actually vanish when added (only strictly true for the sine wave approximation in this example).

Through a linear combination of the known conformational and chemical energy levels of the three enzyme subunits, we tested our hypothesis that a phase shift in combination with some energy transfer between the three units could have a catalytic effect when considered for the global system. Indeed, we can show in Paper 6 that the energy barriers of the rate determining step in ATP synthesis are reduced significantly by roughly one half. Using a straightforward mathematical derivation, we can prove that any similar set of coupled systems of several active sites and energy barriers, provided there exists a mechanism for non-dissipative energy transfer, will exhibit a reduced overall energy barrier (see Figure 17). We therefore coin the concept that ATP synthase may exhibit "phase shift catalysis".

In paper 7, we study the transition dipole moments of p-cresol, a structural analogue of the side chain of tyrosine, using experimental and computational methods. Although tyrosine has been frequently used to determine the partial orientation of proteins, there has not been any systematic study of the absorbance spectra of tyrosine for use in LD spectroscopy. More specifically, neither the transition moment directions, nor how the transition energies are affected by environment had been studied when we, using both experimental and theoretical methods, addressed these problems, including purity of the transitions. Using two kinds of stretched films (polar polyvinyl alcohol and unpolar polyethylene) to orient the p-cresol molecules, the LD spectra could be decomposed into La and Lb (in Platt's terminology) transitions. La and Lb were confirmed to be parallel and perpendicular, respectively, to the geometrical principal axis of the molecule, and to be very pure in character. The transition moment directions were confirmed using quantum mechanical computations.

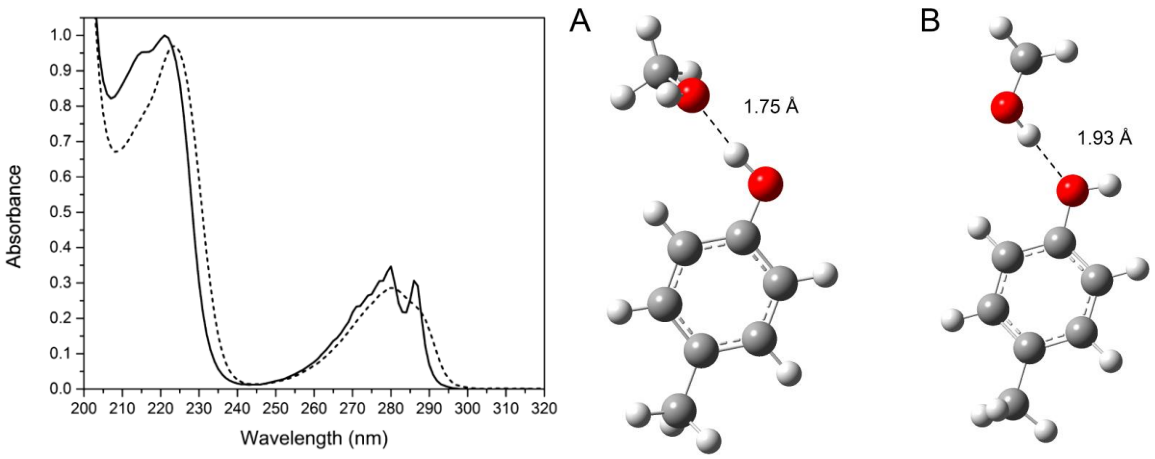

Figure 18. The + 3 nm shift in absorbance of p-cresol dissolved in methanol (dotted line) compared to in cyclohexane, where no hydrogen bonding is available. The calculated and optimized hydrogen bond donating/accepting structures are shown on the right.

Furthermore, p-cresol shows quite different absorption spectra in polar (methanol) and unpolar (cyclohexane) solvents, including a shift in wavelength which could considered to mimic the local environment of a particular tyrosine residue within a protein. As a demonstration, the tyrosines of the recombinase Rad51 were analyzed, assuming that those on the surface of the protein will be exhibiting a shift in wavelength due to an aqueous environment. Using QM calculations, we could show that a + 3 nm shift of the Lb absorption is caused by p-cresol acting as a hydrogen bond donor, and a − 3 nm shift as acceptor (see Figure 18).

An interesting application of the combined transition moment and shift results is the possibility for sensitive detection of variations in environment of proteins. If two tyrosine molecules with different orientations are exposed to different environments, they will give rise to a combined LD spectrum containing minute deviations which can be interpreted in structural terms. Such an effect was recently reported for oriented prion fibers.[90]

5 Conclusions and outlook

In some cases, accepting a theory for being ‘good enough’ in practice may obscure the true theoretical explanation. One example mentioned in this thesis is using hydrogen bonding to explain the stability of DNA helices, a theory good enough to predict DNA melting temperatures, but ignoring the strong hydrophobic attraction which is present between biomolecules in an aqueous environment.

Accepting the role of hydrophobic attractions in stabilizing the B-DNA structure provides for a deeper understanding of the mechanism of DNA strand exchange. In this thesis, it has been shown that a hydrophobic environment created by using PEG as a co-solute increases the rate of strand exchange, and also increases the base pairing accuracy of nucleobases while doing so. Two other important observations are that DNA is not condensed or precipitated, and also that the accelerated exchange is not simply due to melting of the DNA duplexes. Ultimately, the study of a 20-mer DNA duplex model system aims to be generalized to the actual recombinase-mediated recombination *in vivo.* It is a quite striking parallel that both PEG and RecA provide a crowded environment, that base stacking is actively disrupted both in a PEG solution and a RecA filament, and that a B-DNA conformation is maintained in both cases. The similarities between the model system and the real system could lead to a better understanding and that the role of hydrophobic interactions in RecA and Rad51 activity are greater than previously realized.

From another perspective, improving base pairing accuracy and strand exchange rate are also important when manufacturing DNA nanoconstructs which run on DNA fuel, which is becoming an increasingly important field within DNA nanotechnology when compared to static DNA origami products. More results presented in this thesis, that can aid the development of nanotechnology based on biomolecules, as well include the ability to monitor the orientation of DNA nanodevices on a lipid membrane using LD spectroscopy, and the ability to join lipid membranes without the need for exploiting membrane linkers but using only shear force.

Acknowledgements

Upon completing this thesis, I would like to thank my supervisor, prof. Bengt Nordén, for his excellence in science and leadership, and for funding and trusting me from the beginning.

I would also like to thank my co-authors Tamás Beke-Somfai, Louise Fornander, Karolin Frykholm, Erik Lundberg, Amir Mohammadi, Sandra Rocha, prof. Fredrik Westerlund, and prof. Marcus Wilhelmsson, for their collaboration, hard work, and dedication.

Furthermore, I would like to express my gratitude to prof. Anders Blomberg (University of Gothenburg), prof. Tom Brown (University of Oxford), prof. Tommy Gustafsson (Department of Mathematics), Christoph Knuf, prof. Sven Larsson, prof. Per Lincoln, prof. Nicola Markovic, and prof. Björn Åkerman, and my past and current coworkers at the Division of Physical Chemistry, for their advice and help in scientific and practical matters.

Finally, I would like to thank my family and friends for their continuous support during my research and writing.

6 References

1. Allawi HT, SantaLucia J. Thermodynamics of internal C· T mismatches in DNA. *Nucleic acids research* 1998, **26**(11)**:** 2694-2701.

2. Protozanova E, Yakovchuk P, Frank-Kamenetskii MD. Stacked–unstacked equilibrium at the nick site of DNA. *Journal of molecular biology* 2004, **342**(3)**:** 775-785.

3. Kool ET. Hydrogen bonding, base stacking, and steric effects in DNA replication. *Annual review of biophysics and biomolecular structure* 2001, **30**(1)**:** 1-22.

4. Kool ET, Morales JC, Guckian KM. Mimicking the structure and function of DNA: insights into DNA stability and replication. *Angewandte Chemie International Edition* 2000, **39**(6)**:** 990-1009.

5. Yakovchuk P, Protozanova E, Frank-Kamenetskii MD. Base-stacking and base-pairing contributions into thermal stability of the DNA double helix. *Nucleic acids research* 2006, **34**(2)**:** 564-574.

6. Vologodskii AV, Amirikyan B, Lyubchenko YL, Frank-Kamenetskii M. Allowance for heterogeneous stacking in the DNA helix-coil transition theory. *Journal of Biomolecular Structure and Dynamics* 1984, **2**(1)**:** 131-148.

7. Matray TJ, Kool ET. Selective and Stable DNA Base Pairing without Hydrogen Bonds. *J Am Chem Soc* 1998, **120**(24)**:** 6191-6192.

8. Kool ET, Morales JC, Guckian KM. Mimicking the Structure and Function of DNA: Insights into DNA Stability and Replication. *Angew Chem Int Ed Engl* 2000, **39**(6)**:** 990-1009.

9. Bloomfield V, Crothers D, Tinoco Jr I. Nucleic Acids: Structures, Properties, and Functions 2000 Sausalito. *Calif: University Science Books*, **794**.

10. Luo R, Gilson HS, Potter MJ, Gilson MK. The physical basis of nucleic acid base stacking in water. *Biophysical journal* 2001, **80**(1)**:** 140-148.

11. Nielsen PE. Peptide nucleic acids (PNA) in chemical biology and drug discovery. *Chemistry & biodiversity* 2010, **7**(4)**:** 786-804.

12. Martinez CR, Iverson BL. Rethinking the term “pi-stacking”. *Chemical Science* 2012, **3**(7)**:** 2191-2201.

13. Nakano S-i, Oka H, Uotani Y, Uenishi K, Fujii M, Sugimoto N. Stacking interaction in the middle and at the end of a DNA helix studied with non-natural nucleotides. *Molecular BioSystems* 2010, **6**(10)**:** 2023-2029.

14. Guckian KM, Schweitzer BA, Ren RX-F, Sheils CJ, Tahmassebi DC, Kool ET. Factors contributing to aromatic stacking in water: evaluation in the context of DNA. *Journal of the American Chemical Society* 2000, **122**(10)**:** 2213-2222.

15. McDowell JA, Turner DH. Investigation of the structural basis for thermodynamic stabilities of tandem GU mismatches: Solution structure of (rGAG GU CUC) 2 by two-dimensional NMR and simulated annealing. *Biochemistry* 1996, **35**(45)**:** 14077-14089.

16. McDowell JA, He L, Chen X, Turner DH. Investigation of the Structural Basis for Thermodynamic Stabilities of Tandem GU Wobble Pairs: NMR Structures of (rGGA GU UCC) 2 and (rGGA UG UCC) 2. *Biochemistry* 1997, **36**(26)**:** 8030-8038.

17. Poltev V, Shulyupina N. Simulation of interactions between nucleic acid bases by refined atom-atom potential functions. *Journal of Biomolecular Structure and Dynamics* 1986, **3**(4)**:** 739-765.

18. Sponer J, Riley KE, Hobza P. Nature and magnitude of aromatic stacking of nucleic acid bases. *Physical chemistry chemical physics : PCCP* 2008, **10**(19)**:** 2595-2610.

19. Šponer J, Leszczynski J, Hobza P. Nature of nucleic acid-base stacking: nonempirical ab initio and empirical potential characterization of 10 stacked base dimers. Comparison of stacked and H-bonded base pairs. *The Journal of Physical Chemistry* 1996, **100**(13)**:** 5590-5596.

20. Leszczynski J, Hobza P. Hydrogen bonding, stacking and cation binding of DNA bases. *Journal of Molecular Structure: THEOCHEM* 2001, **573**(1)**:** 43-53.

21. Luo R, Gilson HS, Potter MJ, Gilson MK. The physical basis of nucleic acid base stacking in water. *Biophys J* 2001, **80**(1)**:** 140-148.

22. Sponer J, Leszczynski J, Hobza P. Electronic properties, hydrogen bonding, stacking, and cation binding of DNA and RNA bases. *Biopolymers* 2001, **61**(1)**:** 3-31.

23. Yakovchuk P, Protozanova E, Frank-Kamenetskii MD. Base-stacking and base-pairing contributions into thermal stability of the DNA double helix. *Nucleic acids research* 2006, **34**(2)**:** 564-574.

24. Lundberg EP, Feng B, Saeid Mohammadi A, Wilhelmsson LM, Nordén B. Controlling and monitoring orientation of DNA nanoconstructs on lipid surfaces. *Langmuir : the ACS journal of surfaces and colloids* 2012, **29**(1)**:** 285-293.

25. Kogan M, Feng B, Nordén B, Rocha S, Beke-Somfai Ts. Shear-Induced Membrane Fusion in Viscous Solutions. *Langmuir : the ACS journal of surfaces and colloids* 2014, **30**(17)**:** 4875-4878.

26. Beke-Somfai T, Feng B, Nordén B. Energy phase shift as mechanism for catalysis. *Chemical Physics Letters* 2012, **535:** 169-172.

27. Wagner A. *Robustness and evolvability in living systems*. Princeton University Press: Princeton, N.J., 2005.

28. Kunkel TA. DNA replication fidelity. *The Journal of biological chemistry* 1992, **267**(26)**:** 18251-18254.

29. Kibbe WA. OligoCalc: an online oligonucleotide properties calculator. *Nucleic acids research* 2007, **35**(suppl 2)**:** W43-W46.

30. Schütz E, Von Ahsen N. Spreadsheet software for thermodynamic melting point prediction of oligonucleotide hybridization with and without mismatches. *Biotechniques* 1999, **27**(6)**:** 1218-1224.

31. Mao C, Sun W, Shen Z, Seeman NC. A nanomechanical device based on the B-Z transition of DNA. *Nature* 1999, **397**(6715)**:** 144-146.

32. Barish RD, Rothemund PW, Winfree E. Two computational primitives for algorithmic self-assembly: Copying and counting. *Nano letters* 2005, **5**(12)**:** 2586-2592.

33. Stojanovic MN, Semova S, Kolpashchikov D, Macdonald J, Morgan C, Stefanovic D. Deoxyribozyme-based ligase logic gates and their initial circuits. *Journal of the American Chemical Society* 2005, **127**(19)**:** 6914-6915.

34. Yin P, Yan H, Daniell XG, Turberfield AJ, Reif JH. A unidirectional DNA walker that moves autonomously along a track. *Angewandte Chemie International Edition* 2004, **43**(37)**:** 4906-4911.

35. Venkataraman S, Dirks RM, Rothemund PW, Winfree E, Pierce NA. An autonomous polymerization motor powered by DNA hybridization. *Nature Nanotechnology* 2007, **2**(8)**:** 490-494.

36. Bath J, Turberfield AJ. DNA nanomachines. *Nature nanotechnology* 2007, **2**(5)**:** 275-284.

37. He Y, Liu DR. Autonomous multistep organic synthesis in a single isothermal solution mediated by a DNA walker. *Nature nanotechnology* 2010, **5**(11)**:** 778-782.

38. Voigt NV, Tørring T, Rotaru A, Jacobsen MF, Ravnsbæk JB, Subramani R, *et al.* Single-molecule chemical reactions on DNA origami. *Nature nanotechnology* 2010, **5**(3)**:** 200-203.

39. Gu H, Chao J, Xiao S-J, Seeman NC. A proximity-based programmable DNA nanoscale assembly line. *Nature* 2010, **465**(7295)**:** 202-205.

40. Becerril HA, Woolley AT. DNA shadow nanolithography. *Small* 2007, **3**(9)**:** 1534-1538.

41. Surwade SP, Zhao S, Liu H. Molecular lithography through DNA-mediated etching and masking of SiO2. *Journal of the American Chemical Society* 2011, **133**(31)**:** 11868-11871.

42. Lundberg EP, Plesa C, Wilhelmsson LM, Lincoln P, Brown T, Nordén B. Nanofabrication yields. Hybridization and click-fixation of polycyclic DNA nanoassemblies. *ACS nano* 2011, **5**(9)**:** 7565-7575.

43. Tumpane J, Kumar R, Lundberg EP, Sandin P, Gale N, Nandhakumar IS, *et al.* Triplex addressability as a basis for functional DNA nanostructures. *Nano letters* 2007, **7**(12)**:** 3832-3839.

44. Tumpane J, Sandin P, Kumar R, Powers VE, Lundberg EP, Gale N, *et al.* Addressable high-information-density DNA nanostructures. *Chemical physics letters* 2007, **440**(1)**:** 125-129.

45. Zhang DY, Seelig G. Dynamic DNA nanotechnology using strand-displacement reactions. *Nature chemistry* 2011, **3**(2)**:** 103-113.

46. Venkataraman S, Dirks RM, Rothemund PW, Winfree E, Pierce NA. An autonomous polymerization motor powered by DNA hybridization. *Nat Nanotechnol* 2007, **2**(8)**:** 490-494.

47. Turberfield AJ, Mitchell J, Yurke B, Mills Jr AP, Blakey M, Simmel FC. DNA fuel for free-running nanomachines. *Physical review letters* 2003, **90**(11)**:** 118102.

48. Miyoshi D, Sugimoto N. Molecular crowding effects on structure and stability of DNA. *Biochimie* 2008, **90**(7)**:** 1040-1051.

49. Chen Z, Yang H, Pavletich NP. Mechanism of homologous recombination from the RecA-ssDNA/dsDNA structures. *Nature* 2008, **453**(7194)**:** 489-484.

50. Miyoshi D, Matsumura S, Nakano S, Sugimoto N. Duplex dissociation of telomere DNAs induced by molecular crowding. *J Am Chem Soc* 2004, **126**(1)**:** 165-169.

51. Makowski L, Rodi DJ, Mandava S, Minh DD, Gore DB, Fischetti RF. Molecular crowding inhibits intramolecular breathing motions in proteins. *J Mol Biol* 2008, **375**(2)**:** 529-546.

52. Kilburn D, Roh JH, Guo L, Briber RM, Woodson SA. Molecular crowding stabilizes folded RNA structure by the excluded volume effect. *J Am Chem Soc* 2010, **132**(25)**:** 8690-8696.

53. Ellis RJ. Macromolecular crowding: obvious but underappreciated. *Trends Biochem Sci* 2001, **26**(10)**:** 597-604.

54. Sasaki Y, Miyoshi D, Sugimoto N. Effect of molecular crowding on DNA polymerase activity. *Biotechnology journal* 2006, **1**(4)**:** 440-446.

55. Miyoshi D, Karimata H, Sugimoto N. Hydration regulates thermodynamics of G-quadruplex formation under molecular crowding conditions. *J Am Chem Soc* 2006, **128**(24)**:** 7957-7963.

56. Ellis RJ. Macromolecular crowding: obvious but underappreciated. *Trends in biochemical sciences* 2001, **26**(10)**:** 597-604.

57. Minton AP. The influence of macromolecular crowding and macromolecular confinement on biochemical reactions in physiological media. *Journal of biological chemistry* 2001, **276**(14)**:** 10577-10580.

58. Gupta V, Nath S, Chand S. Role of water structure on phase separation in polyelectrolyte–polyethyleneglycol based aqueous two-phase systems. *Polymer* 2002, **43**(11)**:** 3387-3390.

59. Dreesen L, Humbert C, Hollander P, Mani A, Ataka K, Thiry P, *et al.* Study of the water/poly (ethylene glycol) interface by IR-visible sum-frequency generation spectroscopy. *Chemical physics letters* 2001, **333**(5)**:** 327-331.

60. Lüsse S, Arnold K. The interaction of poly (ethylene glycol) with water studied by 1H and 2H NMR relaxation time measurements. *Macromolecules* 1996, **29**(12)**:** 4251-4257.

61. Rajulu AV, Sab PM. Ultrasonic studies of water/poly (ethylene glycol) mixtures. *European polymer journal* 1996, **32**(2)**:** 267-268.

62. Graham N, Chen C. Interaction of poly (ethylene oxide) with solvent—5. The densities of water/poly (ethylene glycol) mixtures. *European polymer journal* 1993, **29**(2)**:** 149-151.

63. De Zutter JK, Knight KL. The hRad51 and RecA proteins show significant differences in cooperative binding to single-stranded DNA. *Journal of molecular biology* 1999, **293**(4)**:** 769-780.

64. McEntee K, Weinstock G, Lehman I. Binding of the recA protein of Escherichia coli to single-and double-stranded DNA. *Journal of Biological Chemistry* 1981, **256**(16)**:** 8835-8844.

65. Cazenave C, Toulme J-J, Helene C. Binding of RecA protein to single-stranded nucleic acids: spectroscopic studies using fluorescent polynucleotides. *The EMBO journal* 1983, **2**(12)**:** 2247.

66. Yoshida M, Muneyuki E, Hisabori T. ATP synthase--a marvellous rotary engine of the cell. *Nature reviews Molecular cell biology* 2001, **2**(9)**:** 669-677.

67. Boyer PD. The ATP synthase--a splendid molecular machine. *Annual review of biochemistry* 1997, **66:** 717-749.

68. Nordén B, Rodger A, Dafforn T, Royal Society of Chemistry (Great Britain). *Linear dichroism and circular dichroism : a textbook on polarized-light spectroscopy*. Royal Society of Chemistry: Cambridge, 2010.

69. Platt JR. Classification of Spectra of Cata-Condensed Hydrocarbons. *The Journal of chemical physics* 1949, **17**(5)**:** 484-495.

70. Norden B, Kurucsev T. Analysing DNA complexes by circular and linear dichroism. *Journal of molecular recognition : JMR* 1994, **7**(2)**:** 141-155.

71. Kim WJ, Akaike T, Maruyama A. DNA strand exchange stimulated by spontaneous complex formation with cationic comb-type copolymer. *Journal of the American Chemical Society* 2002, **124**(43)**:** 12676-12677.

72. Kim WJ, Ishihara T, Akaike T, Maruyama A. Comb-Type Cationic Copolymer Expedites DNA Strand Exchange while Stabilizing DNA Duplex. *Chemistry-A European Journal* 2001, **7**(1)**:** 176-180.

73. Frykholm K, Bombelli FB, Nordén B, Westerlund F. Enhanced DNA strand exchange on positively charged liposomes. *Soft Matter* 2008, **4**(12)**:** 2500-2506.

74. Frykholm K, Nordén B, Westerlund F. Mechanism of DNA strand exchange at liposome surfaces investigated using mismatched DNA. *Langmuir : the ACS journal of surfaces and colloids* 2009, **25**(3)**:** 1606-1611.

75. Reymer A, Frykholm K, Morimatsu K, Takahashi M, Norden B. Structure of human Rad51 protein filament from molecular modeling and site-specific linear dichroism spectroscopy. *Proceedings of the National Academy of Sciences of the United States of America* 2009, **106**(32)**:** 13248-13253.

76. Johansson H-O, Feitosa E, Junior AP. Phase diagrams of the aqueous two-phase systems of poly (ethylene glycol)/sodium polyacrylate/salts. *Polymers* 2011, **3**(1)**:** 587-601.

77. Tejwani RW, Joshi HN, Varia SA, Serajuddin A. Study of phase behavior of poly (ethylene glycol)–polysorbate 80 and poly (ethylene glycol)–polysorbate 80–water mixtures. *Journal of pharmaceutical sciences* 2000, **89**(7)**:** 946-950.

78. Diamond AD, Hsu JT. Protein partitioning in PEG/dextran aqueous two-phase systems. *AIChE Journal* 1990, **36**(7)**:** 1017-1024.

79. Merchuk JC, Andrews BA, Asenjo JA. Aqueous two-phase systems for protein separation: Studies on phase inversion. *Journal of Chromatography B: Biomedical Sciences and Applications* 1998, **711**(1)**:** 285-293.

80. Huddleston JG, Willauer HD, Rogers RD. Phase diagram data for several PEG+ salt aqueous biphasic systems at 25 C. *Journal of Chemical & Engineering Data* 2003, **48**(5)**:** 1230-1236.

81. Ramreddy T, Rao B, Krishnamoorthy G. Site-specific dynamics of strands in ss-and dsDNA as revealed by time-domain fluorescence of 2-aminopurine. *The Journal of Physical Chemistry B* 2007, **111**(20)**:** 5757-5766.

82. Wong K-Y, Pettitt BM. The pathway of oligomeric DNA melting investigated by molecular dynamics simulations. *Biophysical journal* 2008, **95**(12)**:** 5618-5626.

83. Börjesson K, Lundberg EP, Woller JG, Nordén B, Albinsson B. Soft-Surface DNA Nanotechnology: DNA Constructs Anchored and Aligned to Lipid Membrane. *Angewandte Chemie International Edition* 2011, **50**(36)**:** 8312-8315.

84. Tumpane J, Ljungdahl T, Wilhelmsson LM, Nordén B, Brown T, Albinsson B. Membrane-anchored DNA assembly for energy and electron transfer. *Journal of the American Chemical Society* 2009, **131**(8)**:** 2831-2839.

85. Beales PA, Vanderlick TK. Application of nucleic acid-lipid conjugates for the programmable organisation of liposomal modules. *Advances in colloid and interface science* 2014, **207:** 290-305.

86. Beales PA, Nam J, Vanderlick TK. Specific adhesion between DNA-functionalized "Janus" vesicles: size-limited clusters. *Soft Matter* 2011, **7**(5)**:** 1747-1755.

87. Chan Y-HM, van Lengerich B, Boxer SG. Effects of linker sequences on vesicle fusion mediated by lipid-anchored DNA oligonucleotides. *Proceedings of the National Academy of Sciences* 2009, **106**(4)**:** 979-984.

88. Chan Y-HM, van Lengerich B, Boxer SG. Lipid-anchored DNA mediates vesicle fusion as observed by lipid and content mixing. *Biointerphases* 2008, **3**(2)**:** FA17-FA21.

89. Ardhammar M, Lincoln P, Nordén B. Invisible liposomes: refractive index matching with sucrose enables flow dichroism assessment of peptide orientation in lipid vesicle membrane. *Proceedings of the National Academy of Sciences* 2002, **99**(24)**:** 15313-15317.

90. Reymer A, Frederick KK, Rocha S, Beke-Somfai T, Kitts CC, Lindquist S, Nordén B. Orientation of aromatic residues in amyloid cores: Structural insights into prion fiber diversity. *Proceedings of the National Academy of Sciences* 2014, **111**(48)**:** 17158-17163.